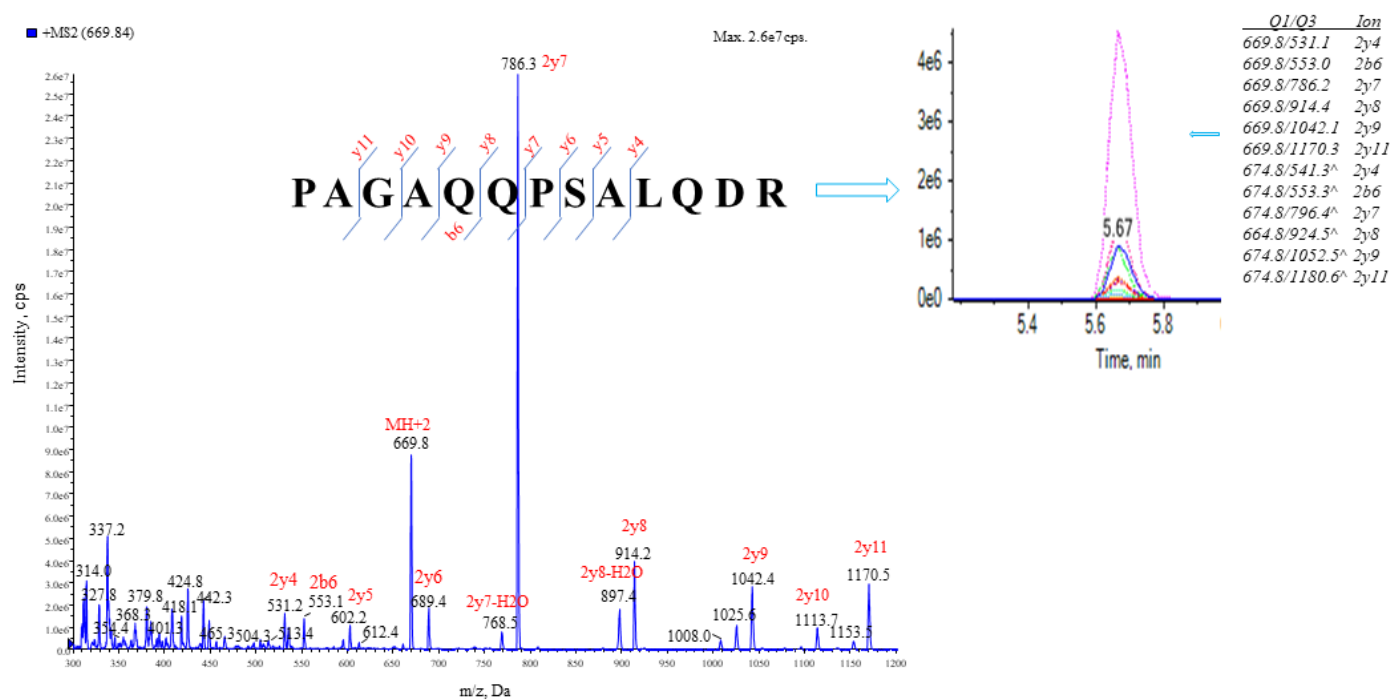


Supplemental Fig 1A

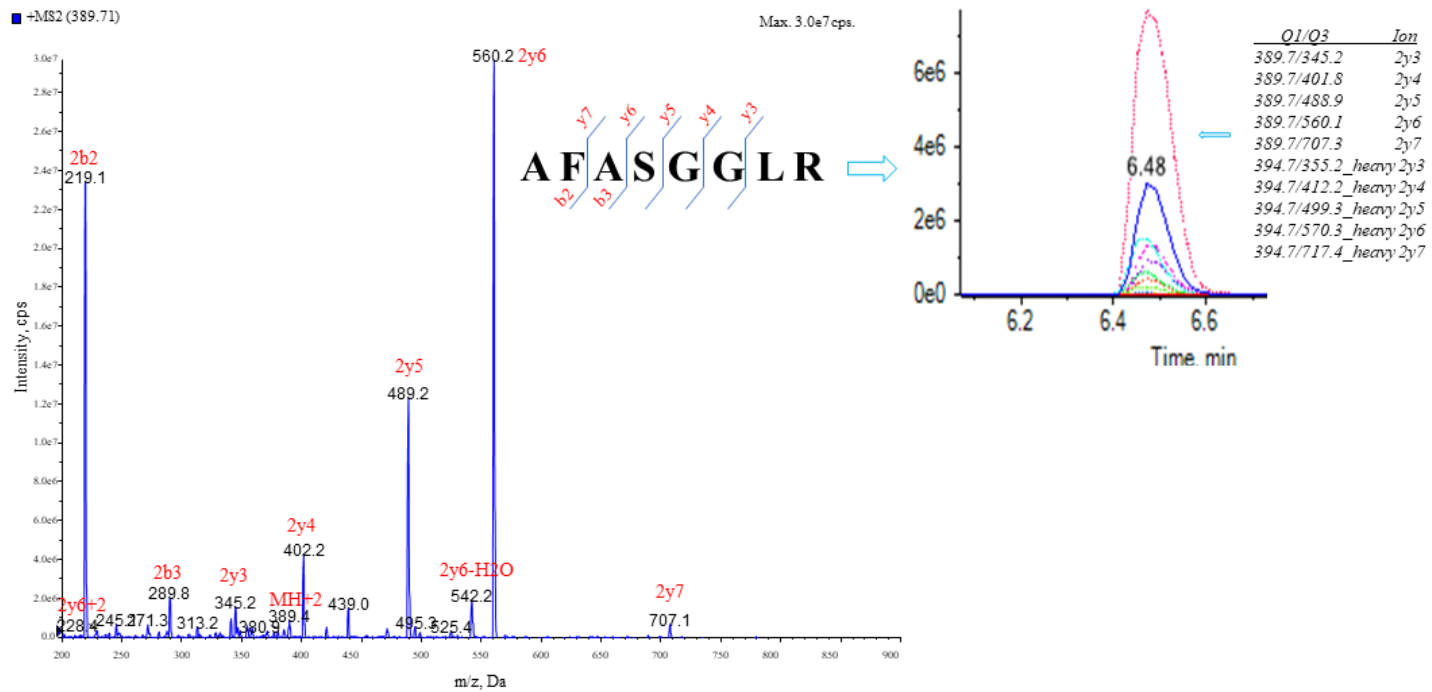
Fragmentation (Q3)



Supplemental Fig 1A: The MS/MS spectra of the peptide pep-U1. Insert: a set of coeluting transition peaks in plasma matrix confirm that the detected SRM signals do derive from the fragment peptide b and y ions and no interfering of co-eluting peaks were present.

Supplemental Fig 1B

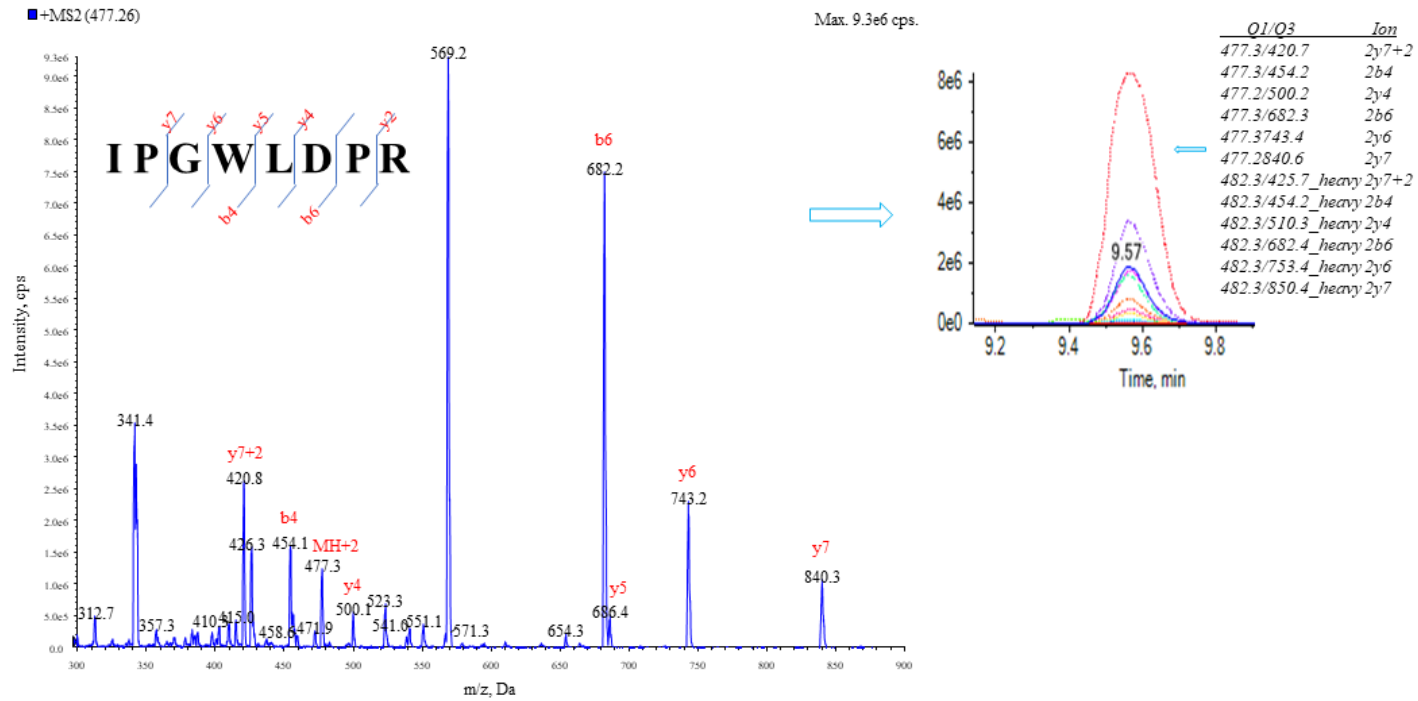
Fragmentation (Q3)



Supplemental Fig 1B: The MS/MS spectra profile of the peptide pep-U2. Insert: a set of coeluting transition peaks in plasma matrix confirm that the detected SRM signals do derive from the fragment peptide b and y ions and no interfering of co-eluting peaks were present.

Supplemental Fig 1C

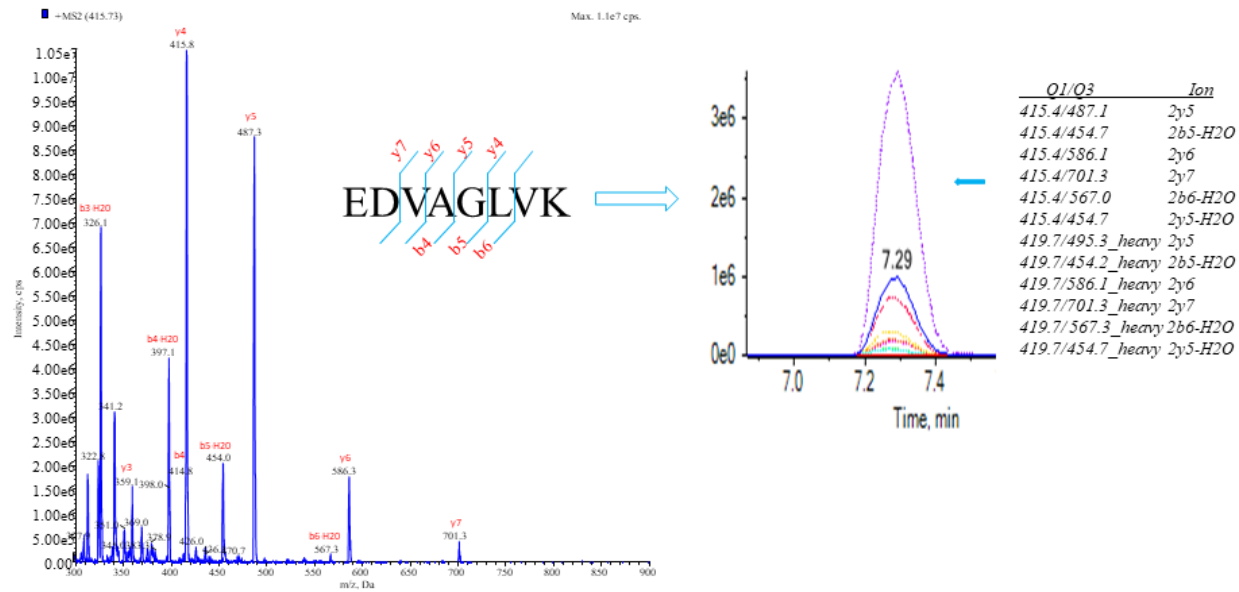
Fragmentation (Q3)



Supplemental Fig 1C: The MS/MS spectra of the peptide pdp-U3. Insert: a set of coeluting transition peaks in plasma matrix confirm that the detected SRM signals do derive from the fragment peptide b and y ions and no interfering of co-eluting peaks were present.

Supplemental Fig 1D

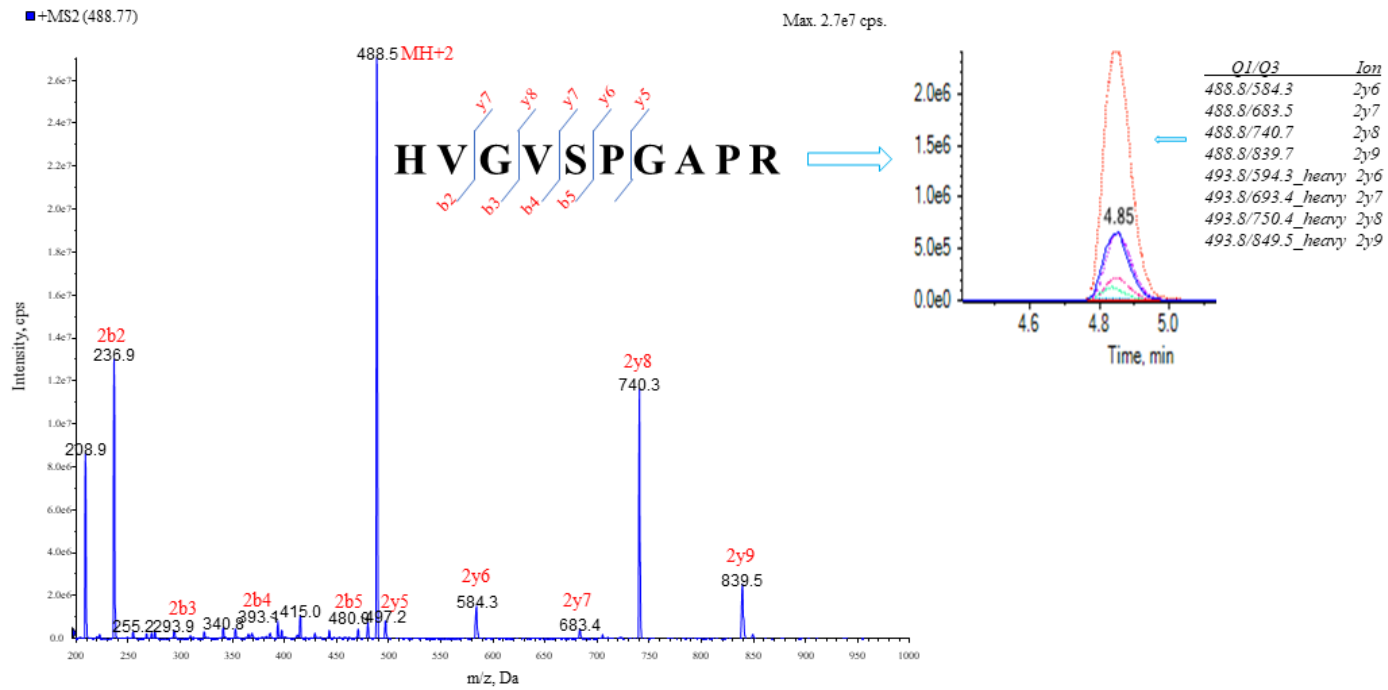
Fragmentation (Q3)



Supplemental Fig 1D: The MS/MS spectra of the peptide pep-U4. Insert: a set of coeluting transition peaks in plasma matrix confirm that the detected SRM signals do derive from the fragment peptide b and y ions and no interfering of co-eluting peaks were present.

Supplemental Fig 1E

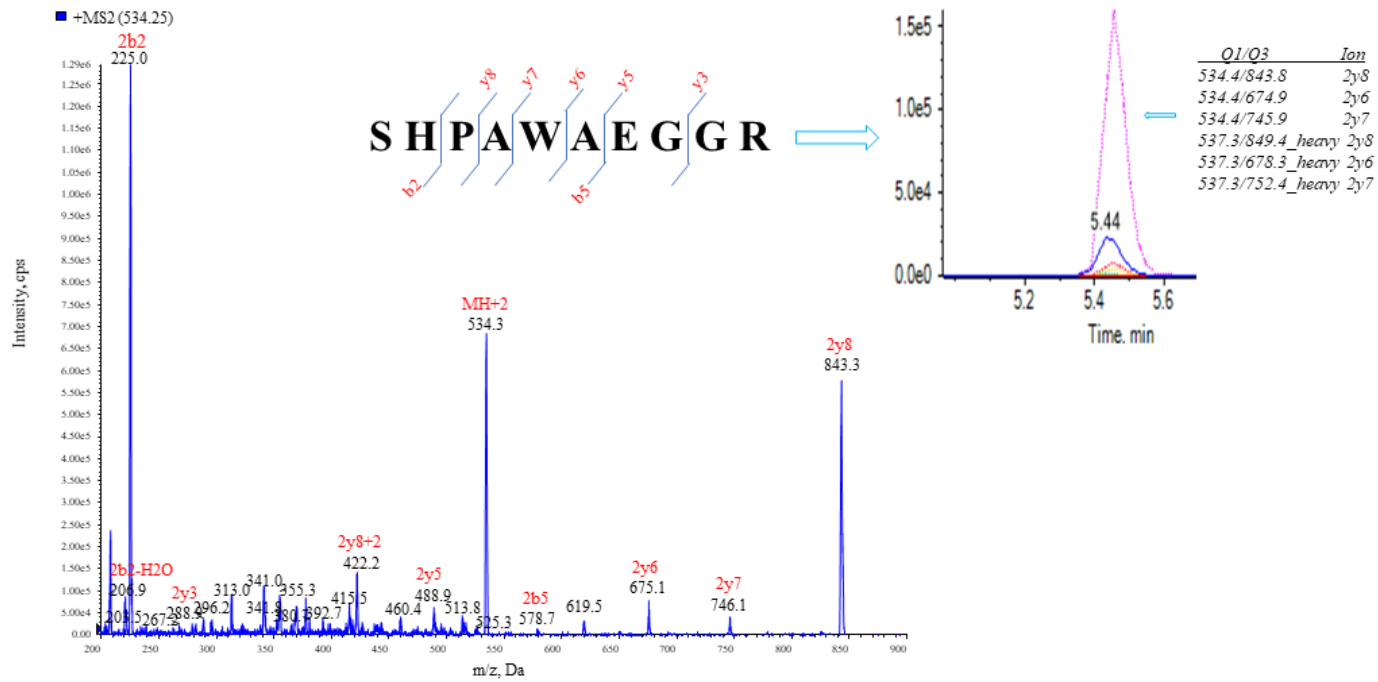
Fragmentation (Q3)



Supplemental Fig 1E: The MS/MS spectra of the peptide pep-U5. Insert: a set of coeluting transition peaks in plasma matrix confirm that the detected SRM signals do derive from the fragment peptide b and y ions and no interfering of co-eluting peaks were present.

Supplemental Fig 1F

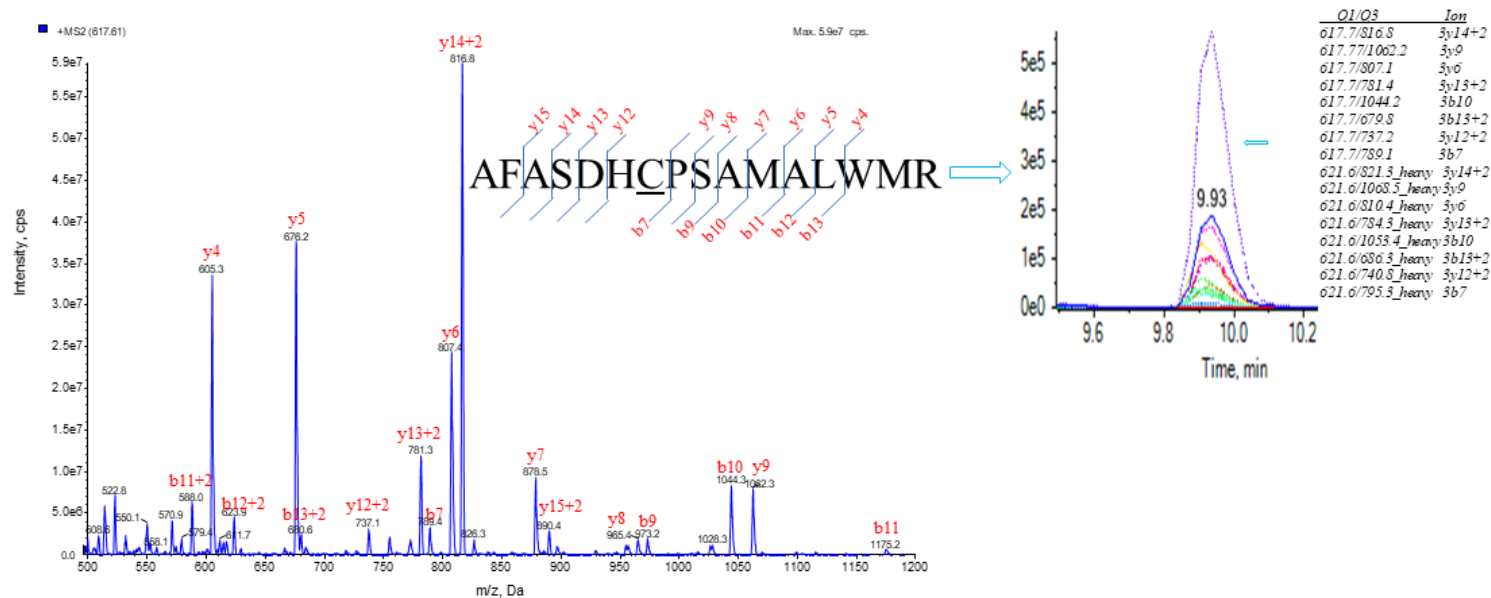
Fragmentation (Q3)



Supplemental Fig 1F: The MS/MS spectra of the peptide pep-UF. Insert: a set of coeluting transition peaks in plasma matrix confirm that the detected SRM signals do derive from the fragment peptide b and y ions and no interfering of co-eluting peaks were present.

Supplemental Fig 1G

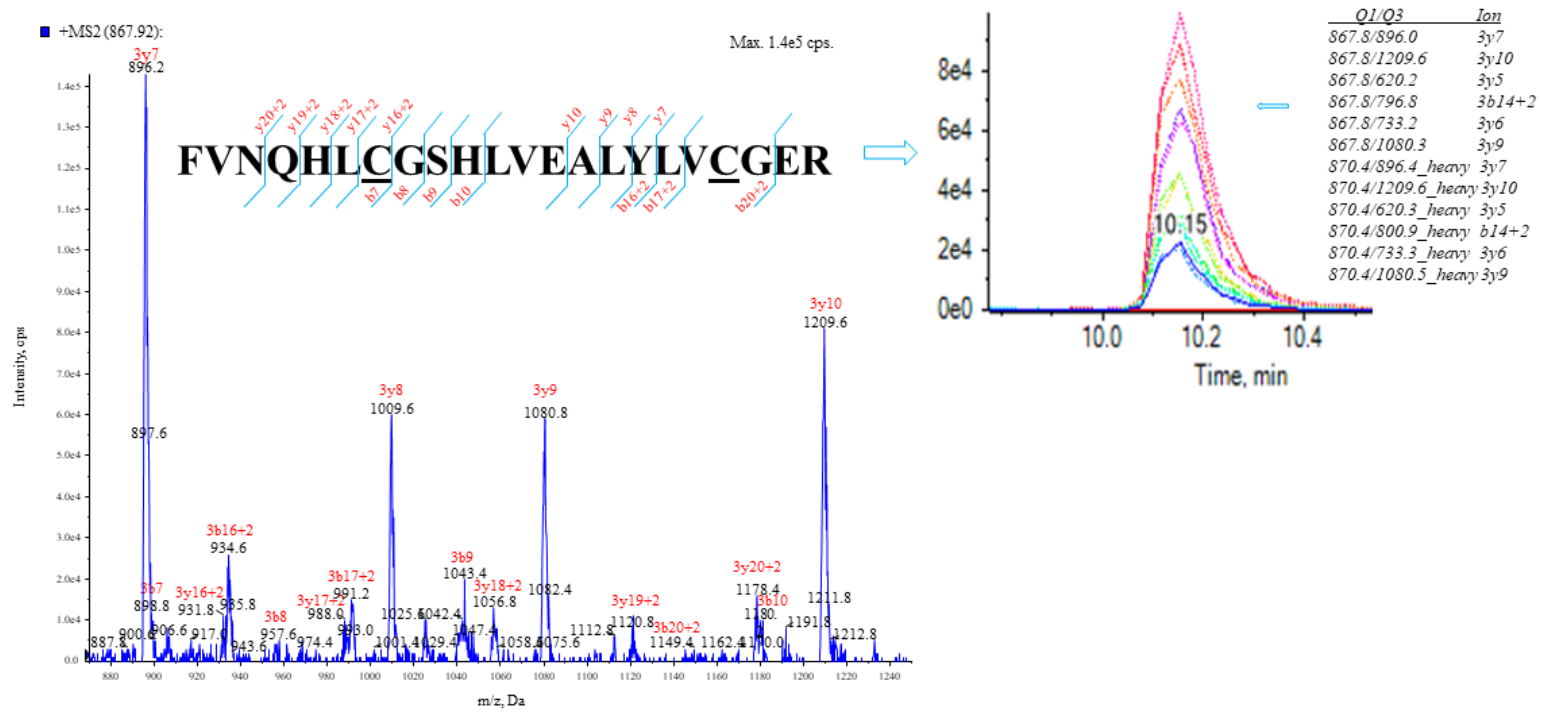
Fragmentation (Q3)



Supplemental Fig 1G: The MS/MS spectra of the peptide pep-US. Insert: a set of coeluting transition peaks in plasma matrix confirm that the detected SRM signals do derive from the fragment peptide b and y ions and no interfering of co-eluting peaks were present. Underlined cysteine residues denote carbamidomethylation (Cys-CAM).

Supplemental Fig 1H

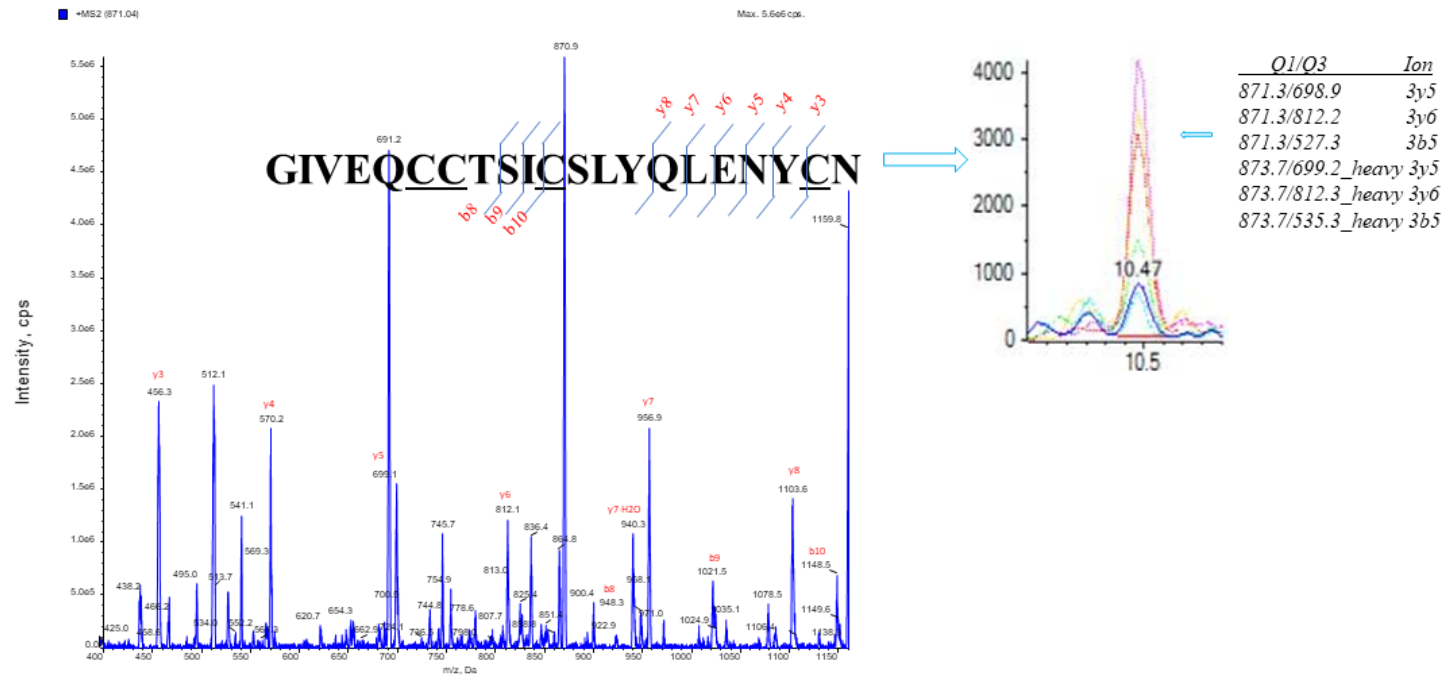
Fragmentation (Q3)



Supplemental Fig 1H: The MS/MS spectra of the target peptide pep-B. Insert: a set of coeluting transition peaks in plasma matrix confirm that the detected SRM signals do derive from the fragment peptide b and y ions and no interfering of co-eluting peaks were present. Underlined cysteine residues denote carbamidomethylation (Cys-CAM).

Supplemental Fig 1I

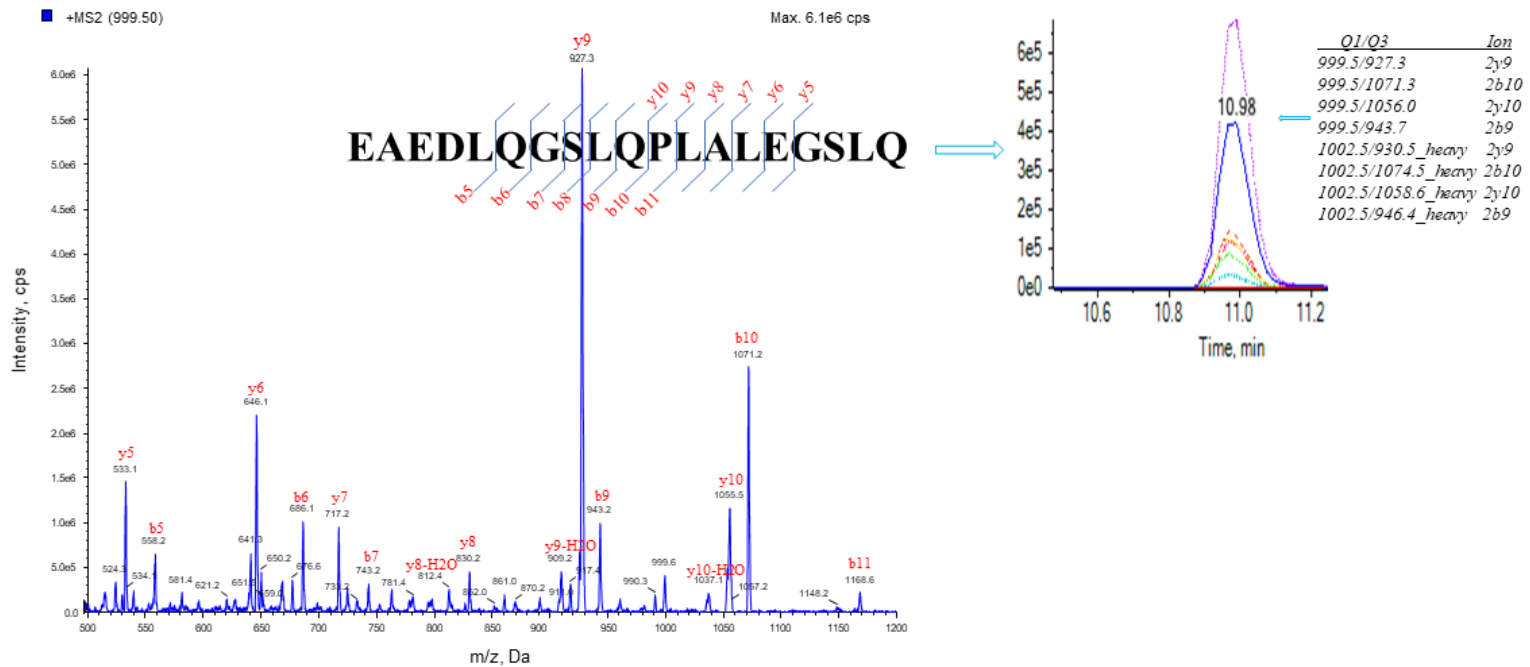
Fragmentation (Q3)



Supplemental Fig 1I: The MS/MS spectra of the peptide pep-A. Insert: a set of coeluting transition peaks in plasma matrix confirm that the detected SRM signals do derive from the fragment peptide b and y ions and no interfering of co-eluting peaks were present. Underlined cysteine residues denote carbamidomethylation (Cys-CAM).

Supplemental Fig 1J

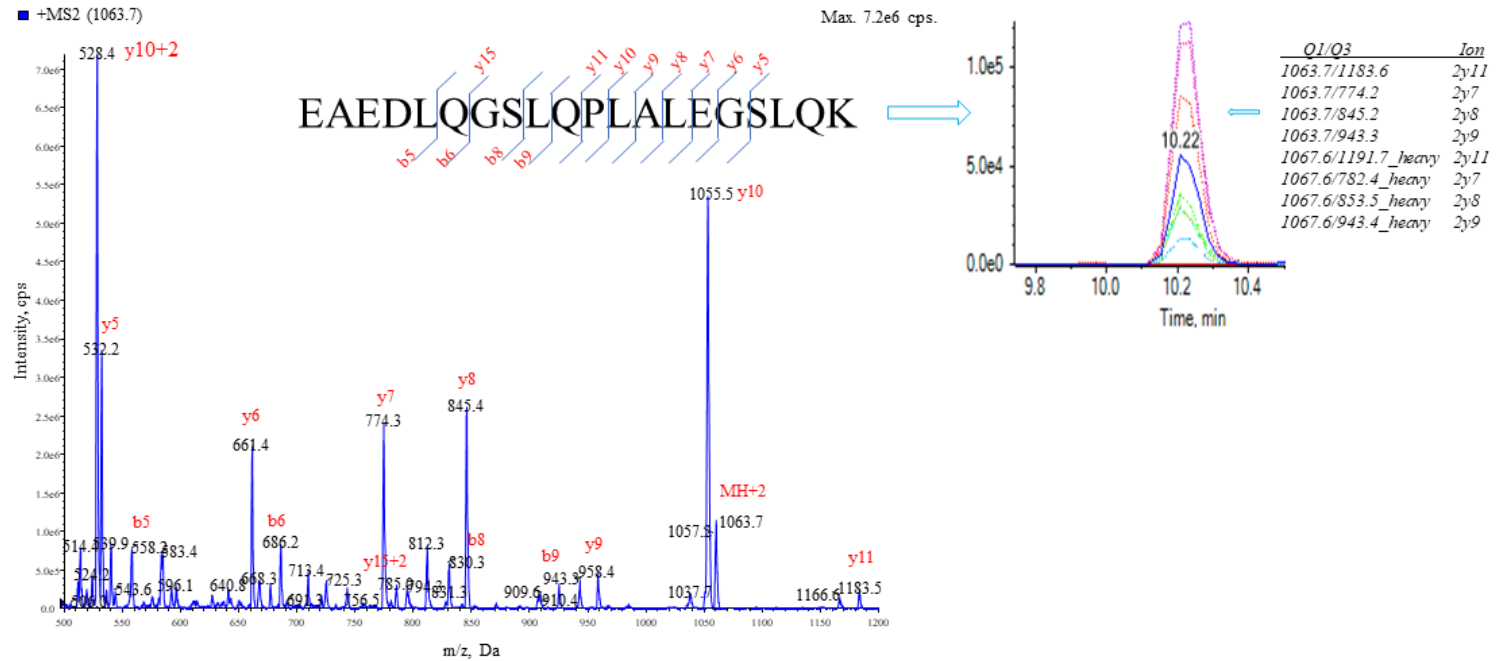
Fragmentation (Q3)



Supplemental Fig 1J: The MS/MS spectra of the peptide PEP- α . Insert: a set of coeluting transition peaks in plasma matrix confirm that the detected SRM signals do derive from the fragment peptide b and y ions and no interfering of co-eluting peaks were present.

Supplemental Fig 1K

Fragmentation (Q3)



Supplemental Fig 1K: The MS/MS spectra profile of the peptide Pep-CaK. Insert: a set of coeluting transition peaks in plasma matrix confirm that the detected SRM signals do derive from the fragment peptide b and y ions and no interfering of co-eluting peaks were present.

Supplemental Fig 2A

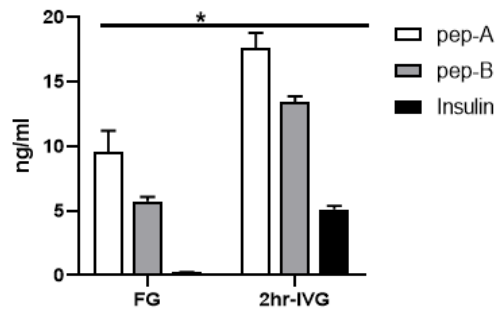
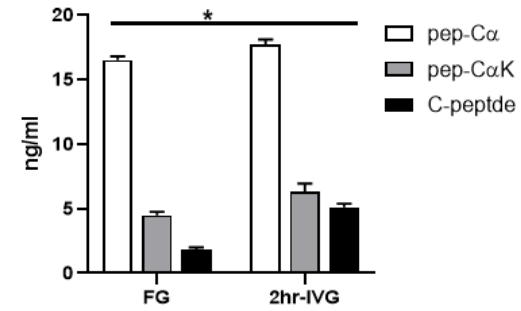


Fig 2B



Supplemental Fig 2: (A) Quantification by SRM-MS of pep-A (A-chain), pep-B (B-chain) and (total) insulin by ELISA; (B) quantification by SRM-MS of processed pep-C (alpha) and non-processed pep-C α K, and C-peptide by ELISA; Plasma was obtained after an overnight fast (FG) and after 2hr-IVG 2-hour continuous intravenous glucose infusion (2 hours: fasting glucose + 98 mg glucose). Asterisk represents significant differences by 2-way ANOVA.

Supplemental Fig 3A

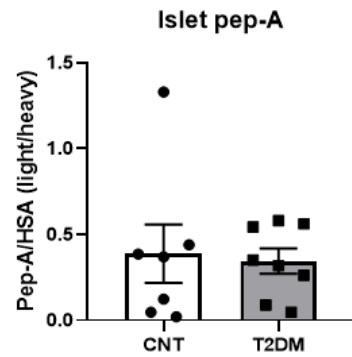


Fig 3B

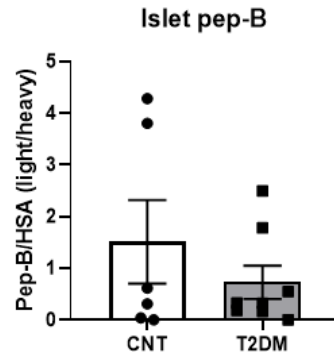
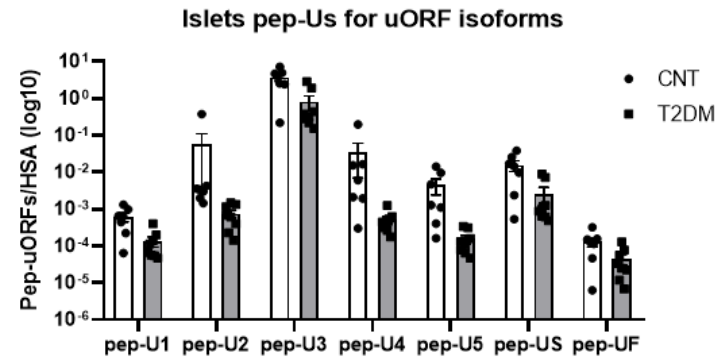


Fig 3C



Supplemental Fig 3: SRM –MS quantification of A-chain (A) and B-chain (B) in human islets of control (CNT) and T2DM samples. Y axis represents endogenous pep-A and pep-B transition peak areas normalized with those of respective isotope-labeled tryptic peptides.

Supplemental Fig 4A

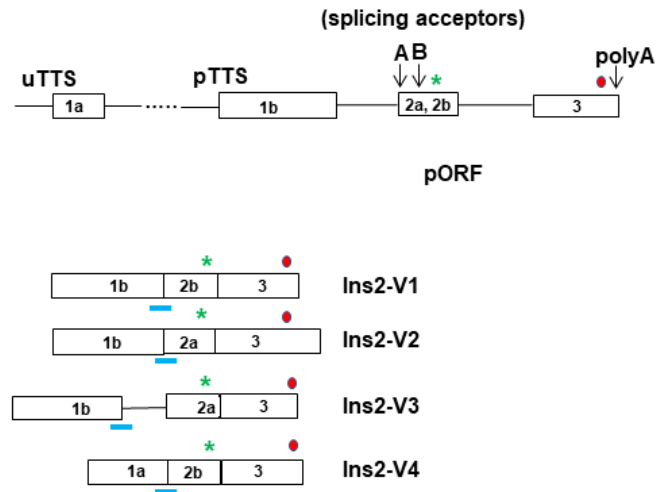
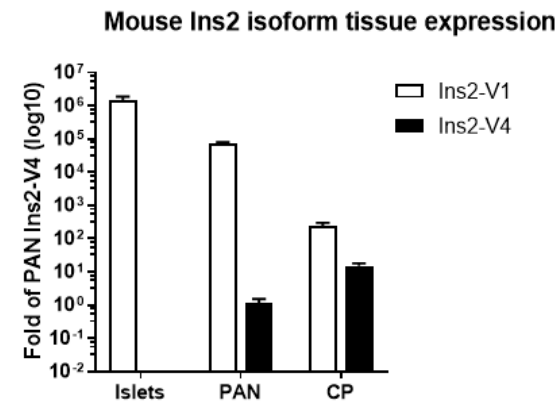


Fig 4B



Supplemental Figure 4: (A): mouse *Ins2* gene structures and their alternatively spliced isoforms. uTSS, upstream transcription start site; pTSS, primary transcription start site. Open boxes represent exons and solid lines represent introns. Downward arrows and capital letters are at exon-2 and polyadenylation sites. Green asterisk represents translation initiation codon and red dot stop codon. (B): TaqMan RT-qPCR of mouse *Ins2* uTSS and pTSS isoforms, Ins2-V1 and Ins2-V4, in islets, PAN (pancreas), and CP (choroid plexus). Ins2-V1 isoform mRNA was found in mouse islets to be more than 10⁵-fold higher than in CP, and 10⁸-fold higher than Ins2-V4.

Islet isolation centre	The Scharp-Lacy Research Institute	University of Wisconsin	University of Pennsylvania	University of Miami	University of Pennsylvania			
Donor history of diabetes? Yes/No	No	No	Yes	No	No	No	No	No
If Yes, complete the next two lines if this information is available								
Diabetes duration (years)			0-5 years					
Glucose-lowering therapy at time of death ^c			Oral medication					

RECOMMENDED INFORMATION								
Donor cause of death	Head trauma	Anoxia	Stroke	Head trauma	Stroke	Anoxia	Stroke	Head trauma
Warm ischaemia time (h)	0.4	0	0	0	0	0	0	0
Cold ischaemia time (h)	12.8	6.2	9.9	14.5	4.2	7.4	12.0	6.9
Estimated purity (%)	95%	95%	90%	90%	95%	95%	80%	94%
Estimated viability (%)	95%	95%	95%	95%	95%	90%	93%	94%
Total culture time (h) ^d	38	82	95	96	48	22	96	42

Glucose-stimulated insulin secretion or other functional measurement ^e	3.9 SI	NA						
Handpicked to purity? Yes/No	Yes	Yes	Yes	Yes	Yes	Yes	Yes	Yes
Additional notes								

^aIf you have used more than eight islet preparations, please complete additional forms as necessary

^bFor example, IIDP, ECIT, Alberta IsletCore

^cPlease specify the therapy/therapies

^dTime of islet culture at the isolation centre, during shipment and at the receiving laboratory

^ePlease specify the test and the results

Islet preparation	9	10	11	12	13	14	15	16
MANDATORY INFORMATION								
Unique identifier	SAMN08768790	SAMN08768788	SAMN08768784	SAMN08768979	SAMN08768974	SAMN08768973	SAMN08768971	SAMN08768972
Donor age (years)	51	46	52	59	28	45	61	27
Donor sex (M/F)	F	F	F	M	M	M	M	M
Donor BMI (kg/m ²)	22.5	35.9	42.8	27.7	29.2	36.4	27.0	30
Donor HbA _{1c} or other measure of blood glucose control	179.60 mg/dl	262.40 mg/dl A1c=6.8	237.40 mg/dl A1c=6.6	199.80 mg/dl A1c=6.5	232.00 mg/dl	174.00 mg/dl	146.40 mg/dl	108.00 mg/dl

Origin/source of islets ^b	IIDP	IIDP	IIDP	IIDP	IIDP	IIDP	IIDP	IIDP
Islet isolation centre	The Scharp-Lacy Research Institute	University of Pennsylvania	The Scharp-Lacy Research Institute	The Scharp-Lacy Research Institute	University of Wisconsin	University of Wisconsin	Southern California Islet Cell Resource Center	University of Wisconsin
Donor history of diabetes? Yes/No	No	Yes	Yes	Yes	No	No	No	No
If Yes, complete the next two lines if this information is available								
Diabetes duration (years)		0-5 years	0-5 years	6-10 years				
Glucose-lowering therapy at time of death ^c		Oral medication	Oral medication	Oral medication				

RECOMMENDED INFORMATION								
Donor cause of death	Stroke	Stroke	Stroke	Stroke	Head trauma	Stroke	Head trauma	Head trauma
Warm ischaemia time (h)	0	0	0	0	0	0	0	0.53
Cold ischaemia time (h)	11.3	6.9	6.9	6.1	3.5	9	Not documented	4.3
Estimated purity (%)	95%	50%	90%	85%	85%	90%	80%	95%
Estimated viability (%)	95%	92%	95%	95%	98%	93%	98%	99%

Total culture time (h) ^d	111	18	68	59	66	24	70	43
Glucose-stimulated insulin secretion or other functional measurement ^e	NA							
Handpicked to purity? Yes/No	Yes							
Additional notes								

Islet preparation	17	18	19	20	21	22		
MANDATORY INFORMATION								
Unique identifier	SAMN08768992	SAMN08769032	SAMN08769026	SAMN08616281	SAMN08617637	SAMN10229738		
Donor age (years)	16	26	37	45	54	46		
Donor sex (M/F)	M	M	F	M	M	F		
Donor BMI (kg/m ²)	31.5	28.7	38.1	27.2	24.5	33.2		
Donor HbA _{1c} or other measure of blood glucose control	209.20 mg/dl	142.00 mg/dl A1c=6.5	253.80 mg/dl A1c=8.2	246.00 mg/dl A1c=6.5	122.40 mg/dl A1c=4.8	164.20 mg/dl A1c=10.7		
Origin/source of islets ^b	IIDP	IIDP	IIDP	IIDP	IIDP	IIDP		
Islet isolation centre	University of Pennsylvania	The Scharp-Lacy Research Institute	University of Pennsylvania	University of Wisconsin	University of Wisconsin	Southern California Islet Cell Resources Center		
Donor history of diabetes? Yes/No	No	Yes	Yes	Yes	Yes	Yes		
If Yes, complete the next two lines if this information is available								
Diabetes duration (years)		0-5 years	0-5 years	0-5 years	6 years	>10 years		
Glucose-lowering therapy at time of death ^c		Oral medication	Oral medication	Oral medication	Oral medication	Insulin 20 units		

RECOMMENDED INFORMATION

Donor cause of death	Anoxia	Head trauma	Stroke	Stroke	Stroke	Stroke		
Warm ischaemia time (h)	0	0	0	0	0	0		
Cold ischaemia time (h)	9.4	7.3	4.7	11.4	10.1	5.8		
Estimated purity (%)	70%	90%	85%	85%	80%	95%		
Estimated viability (%)	95%	95%	94%	95%	92%	95%		
Total culture time (h) ^d	21	55	22	101	18	30		
Glucose-stimulated insulin secretion or other functional measurement ^e	NA	NA	NA	NA	NA	NA		
Handpicked to purity? Yes/No	Yes	Yes	Yes	Yes	Yes	Yes		
Additional notes								

Supplemental Table 2: Clinical data of human postmortem choroid plexus (PMI: postmortem interval; RIN: RNA integrity number; BMI: body mass index; ASCVD: Arteriosclerotic Hypertensive Cardiovascular Disease; COPD: Chronic Obstructive Pulmonary Disease; ND: No Diagnosis).

Age	Sex	Race	PMI	Ph	RIN	Smoker	BMI	Axis III	Cause of Death
35.9	Male	African American	49.5	5.88	4.2	No	19.1	Diabetes Mellitus, Type I, (IDDM), N.D.	THREE VESSEL OCCLUSIVE CORONARY ATHEROSCLEROSIS
56.3	Male	African American	31.5	6.09	NA	Unknown	31.3	Diabetes Mellitus, Type I, (IDDM), N.D.	PULMONARY EMBOLISM DUE TO DEEP VENOUS THROMBOSIS
61.2	Female	Caucasian	24.5	5.99	5.9	No	31.4	Diabetes Mellitus, Type I, (IDDM) N.D.	CORONARY ATHEROSCLEROSIS
48.5	Female	African American	23.5	6.25	5.9	Unknown	26.9	Diabetes Mellitus, Type I, (IDDM), Hypertension	SEVERE GENERALIZED ATHEROSCLEROSIS DUE TO HYPERTENSION
41.5	Male	Caucasian	34.5	6.47	8.4	No	27.2	Diabetes Mellitus, Type I, (IDDM), ASHCVD	ATHEROSCLEROTIC CARDIOVASCULAR DISEASE
84.2	Male	African American	27.5	6.27	NA	No	41.2	Diabetes Mellitus, Type I, (IDDM), COPD	MULTIPLE BLUNT IMPACT INJURIES
41.1	Male	African American	55.5	6.73	NA	No	24.1	Diabetes Mellitus, Type II (Non-IDDM), Hypertension	HYPERTENSIVE CARDIOVASCULAR DISEASE WITH BIVENTRICULAR DIALA
41.2	Female	African American	32	6.62	8.9	Yes	27.4	Diabetes Mellitus, Type II (Non-IDDM), Hypertension	ASHCVD WITH CORONARY ARTERY STENOSIS
54.9	Male	African American	27	6.11	8.4	No	42.1	Diabetes Mellitus, Type II (Non-IDDM), Hypertension	PULMONARY EMBOLUS DUE TO DEEP VENOUS THROMBOSIS
56.5	Male	African American	24	6.51	8.9	No	40.3	Diabetes Mellitus, Type II (Non-IDDM), Hypertension	PULMONARY EMBOLUS DUE TO DEEP VENOUS THROMBOSIS
27.6	Female	African American	21	6.41	8.3	No	52	Non-Diabetes, Obesity	ARRHYTHMOGENIC RIGHT VENTRICULAR DYSPLASIA
45.3	Male	African American	21.5	6.73	8.1	No	68.9	Non-Diabetes, Obesity	HYPERTENSIVE CARDIOVASCULAR DISEASE AND MORBID OBESITY
52.6	Female	African American	26	6.38	9.1	No	36.9	Non-Diabetes, Obesity	ACUTE FIBRINOUS PERICARDITIS WITH CARDIAC TAMPONADE
66.7	Female	Caucasian	29.5	6.48	7	No	40.3	Non-Diabetes, Obesity	RUPTURED THORACIC AORTIC ANEURYSM
45.4	Female	African American	43	6.43	8.1	No	21.9	Non-Diabetes, Normal	RUPTURED DISSECTING THORACIC AORTIC ANEURYSM

Supplemental Table 3: Clinical data of human postmortem choroid plexus (PMI: postmortem interval; RIN: RNA integrity number; BMI: body mass index)

Supplemental Table 3: TaqMan probe and primer sequences of human *INS*, mouse *Ins2* isoforms, the autoantigen and insulin differentiation factor gene expression assay IDs (probe sequences are proprietary of Thermo Fisher Scientific).

Isoforms	TaqMan probe	Forward primer	Reverse primer
Exon-2	TGAACCAACACCTGTGCG	CCCAGCCGCAGCCTTT	AGAGAGCTTCCACCAGGTGTGA
INS3A	Hs00355773_m1 (NM_000207)	Exon-2	Exon-3A (junction 126 bp amplicon)
EX2-I2	ACGAGGCTTCTTCTACACAC	TCACACCTGGTGGGAAGCTCTCT	GGCAGCAATGGGCAGTTG
INS1A	CCATCAAGCAGATCACTGT	GGACAGGCTGCATCAGAAGAG	ACAGGGCCATGGCAGAAG
INS1B	TTTGCCTCAGATCACT	CCATCAAGCAGGTCTGTTCCA	GGGCCATGGCAGAAGGA
INS1C	ACCCAGATCACTGTC	CCATCAAGCAGGTCTGTTCCA	GCAGGAGGCCGCATCCA
INS1I	CCATCAAGCAGGTCTG	GGACAGGCTGCATCAGAAGAG	AGCCACCTGACGCAAAG
INSUA	CCATCAAGCAGATCACTGT	GGGAGATGGGCTCTGAGACTATAA	ACAGGGCCATGGCAGAAG
INSUB	TTTGCCTCAGATCACT	GGGAGATGGGCTCTGAGACTATAA	GGGCCATGGCAGAAGGA
INSUC	ACCCAGATCACTGTC	GGGAGATGGGCTCTGAGACTATAA	GCAGGAGGCCGCATCCA
INSU1	CCATCAAGCAGGTCTG	GGGAGATGGGCTCTGAGACTATAA	AGCCACCTGACGCAAAG
INS3B	CAGGCTGCCCTGCAG	TAGAGGGAGCAGATGCTGGTACA	AGGCTTCTTCTACACACCCAAGA
Ins2-V1	CAAGCAGGAAGGTTATTGT	CCGCTACAATCAAAAACCATCA	CATCCACAGGGCCATGTTG
Ins2-V2	CAAGCAGGAAGGTACTC	CCGCTACAATCAAAAACCATCA	GAGCCAGGCCCACTGAGA
Ins2-V3	ATCCGCTACAATCAA	CCAGTAACCACCAGCCCTAAGT	AGATAGGCTTCTGCTTGCTGATG
Ins2-V4	CTGGAGGTTATTGTTTCAA	GCTCCTACGCTGAAATTCCAA	AAGGTGCTGCTTGACAAAAGC
IGF1	Hs01547656_m1 (NM_000618)	exon-2	exon-3 (junction 68 bp amplicon)
GAD2	Hs00609534_m1 (NM_000818)	exon-15	exon-16 (junction 95 bp amplicon)
PTPRN	Hs00160947_m1 (NM_001199763)	exon-3	exon-4 (junction 65 bp amplicon)
SLC30A8	Hs00545183_m1 (NM_001172811)	exon-5	exon-6 (junction 73 bp amplicon)
ICA1	Hs01119158_m1 (NM_001136020)	exon-13	exon-14 (junction 77 bp amplicon)
MAFA	Hs01651425_s1 (NM_201589)	exon-1	exon-1 (exon-1 121 bp amplicon)
NEUROD1	Hs01922995_s1 (NM_002500)	exon-2	exon-2 (exon-2 110 bp amplicon)
ISL1	Hs00158126_m1 (NM_002202)	exon-5	exon-6 (junction 57 bp amplicon)
NKX6-1	Hs00232355_m1 (NM_006168)	exon-1	exon-2 (junction 93 bp amplicon)
PDX1	Hs00236830_m1 (NM_000209)	exon-1	exon-2 (junction 73 bp amplicon)
PAX4	Hs00173014_m1 (NM_006193)	exon-6	exon-7 (junction 115 bp amplicon)
NEUROG3	Hs01875204_s1 (NM_020999)	exon-2	exon-2 (exon-2 117 bp amplicon)

Supplemental Table 4: unlabeled and isotope-labeled (marked by asterisk) tryptic peptide sequences and their molecular weights (MW; dal, Dalton) for SRM-MS assay. CAM in the peptide sequences represents carbamidomethylation of cysteine residues to block its oxidation, and (*) the isotope labeled amino acid residues (hydrogen-2 for V and A, carbon-13 and nitrogen-15 for K, R and F).

Peptide name	Peptide sequences	MW (dal)	AA
pep-B1	H ₂ N-FVNQHLC[CAM]GSHLVEALYLVC[CAM]GER-OH	2601.27	22
pep-B2	H ₂ N-GFFYTPK-OH	859.43	7
pep-A	H ₂ N-GIVEQC[CAM]C[CAM]TSIC[CAM]SLYQLENYC[CAM]N-OH	2611.10	21
pep-C α	H ₂ N-EAEDLQGSLQPLALEGSLQ-OH	1998.00	19
pep-C α K	H ₂ N-EAEDLQGSLQPLALEGSLQK-OH	2126.10	20
pep-U1	H ₂ N-PAGAQQPSALQDR-OH	1338.67	13
pep-U2	H ₂ N-AFASGGLR-OH	778.42	8
pep-U3	H ₂ N-IPGWLDPR-OH	953.52	8
pep-U4	H ₂ N-EDVAGLVK-OH	830.46	8
pep-U5	H ₂ N-HVGVSPGAPR-OH	976.53	10
pep-US	H ₂ N-AFASDHC[CAM]PSAMALWMR-OH	1850.81	16
pep-UF	H ₂ N-SHPAWAEGGR-OH	1067.50	10
pep-B1*	H ₂ N-FV ² NQHLC[CAM]GSHLVEALYLVC[CAM]GER-OH	2609.23	22
pep-B2*	H ₂ N-GF ² F ¹³ YTPK-OH	867.00	7
pep-A*	H ₂ N-GIV ² EQC[CAM]C[CAM]TSIC[CAM]SLYQLENYC[CAM]N-OH	2619.01	21
pep-C α *	H ₂ N-EA ² EDLQGSLQPLA ¹³ LEGSLQ-OH	2004.00	19
pep-C α K*	H ₂ N-EAEDLQGSLQPLALEGSLQK ¹⁵ -OH	2134.10	20
pep-U1*	H ₂ N-PAGAQQPSALQDR ¹³ -OH	1348.00	13
pep-U2*	H ₂ N-AFASGGLR ¹³ -OH	788.42	8
pep-U3*	H ₂ N-IPGWLDPR ¹³ -OH	963.00	8
pep-U4*	H ₂ N-EDVAGKVK ¹³ -OH	838.46	8
pep-U5*	H ₂ N-HVGVSPGAPR ¹³ -OH	986.53	10
pep-US*	H ₂ N-A ¹³ FA ¹⁵ SDHC[CAM]PSA ¹³ MA ¹⁵ LWMR-OH	1862.00	16
pep-UF*	SHPA ¹³ WA ¹⁵ EGGR-OH	1073.14	10

Supplemental Table 5: quantitation validation of SRM-MS assay in pooled postmortem cerebrum

Target peptide	SRM			
	^a Linear Regression and R ²	^b LOQ (nM)	CV (%)	^c Accuracy (mean±SD, %)
Pep-B	$\log_2 \text{Con}(\text{nM}) = 7.035 + 0.946 * \log_2 \text{Pep-B1}(\text{ratio, L/H}); R^2 = .998$	0.59	3.22	100.54±9.12
Pep-A	$\log_2 \text{Con}(\text{nM}) = 9.685 + 1.065 * \log_2 \text{Pep-A}(\text{ratio, L/H}); R^2 = .998$	4.69	7.03	101.11±6.40
Pep-Cα	$\log_2 \text{Con}(\text{nM}) = 7.51 + 1.04 * \log_2 \text{Pep-Cα}(\text{ratio, L/H}); R^2 = .997$	6.25	3.43	98.28±8.76
Pep-CαK	$\log_2 \text{Con}(\text{nM}) = 7.32 + 0.97 * \log_2 \text{Pep-CαK}(\text{ratio, L/H}); R^2 = .999$	0.26	3.56	100.28±6.60
Pep-U1	$\log_2 \text{Con}(\text{nM}) = 7.636 + 1.017 * \log_2 \text{Pep-U1}(\text{ratio, L/H}); R^2 = 1$	0.38	2.04	100.23±5.53
Pep-U3	$\log_2 \text{Con}(\text{nM}) = 6.926 + 1.031 * \log_2 \text{Pep-U3}(\text{ratio, L/H}); R^2 = .999$	3.32	0.81	100.26±7.43
Pep-U4	$\log_2 \text{Con}(\text{nM}) = 10.655 + 1.02 * \log_2 \text{Pep-U4}(\text{ratio, L/H}); R^2 = .998$	2.34	3.34	100.39±10.08
Pep-UF	$\log_2 \text{Con}(\text{nM}) = 7.519 + 0.991 * \log_2 \text{Pep-UF}(\text{ratio, L/H}); R^2 = .999$	0.21	5.95	100.40±8.57
Pep-US	$\log_2 \text{Con}(\text{nM}) = 8.257 + .929 * \log_2 \text{Pep-US}(\text{ratio, L/H}); R^2 = .998$	7.81	2.87	100.30±8.57

^a Linearity was determined by linear regression between measured concentration and peak area ratio (L/H) versus theoretical concentration determined by Light-SIS peptides (unlabeled form). All output of MultiQuant were weighted by $1/\chi^2$. Sum of all transition peak area ratio (L/H) to get peak area ratio at the peptide level.

^b LOQ was determined from the standard curve, defined as the lowest limits of quantification calibrated with acceptable CV<20% and accuracy within 100±20%.

^c Accuracy was estimated by back fitting data to the STD curve and average recovery from all quantified points in the plots. Data are mean±SD (%). Calibration curve is based on internal standard (IS unlabeled form) concentration and peak area ratio (transition ion peak area/IS peak area) and prepared in a pooled plasma matrix which was prepared from studying plasma samples >=5 points.

Supplemental Table 6: quantitation validation of SRM-MS assay in pooled human plasma

Target peptide	SRM			
	^a Linear Regression and R2	^b LOQ ng/ml	CV (%)	^c Accuracy (%)
Pep-B	$\log_2\text{Con}(\text{ng/ml}) = 6.8 + 0.94 * \log_2\text{Pep-B1, ratio (L/H)}; R^2 = .998$	1.52	3.77	100.36±9.74
Pep-A	$\log_2\text{Con}(\text{ng/ml}) = 8.72 + 0.67 * \log_2\text{Pep-A, ratio (L/H)}; R^2 = .998$	6.12	12.40	100.46±9.87
Pep-CaK	$\log_2\text{Con}(\text{ng/ml}) = 7.118 + .942 * \log_2\text{Pep-CaK, ratio (L/H)}; R^2 = .999$	3.32	3.20	100.15±5.46
Pep-Ca	$\log_2\text{Con}(\text{ng/ml}) = 7.256 + .903 * \log_2\text{Pep-Ca, ratio (L/H)}; R^2 = .999$	4.10	1.30	100.13±5.36
Pep-U1	$\log_2\text{Con}(\text{ng/ml}) = 5.926 + .988 * \log_2\text{Pep-U1, ratio (L/H)}; R^2 = 1$	1.01	1.14	100.13±4.86
Pep-U2	$\log_2\text{Con}(\text{ng/ml}) = 4.43 + 1.046 * \log_2\text{PepU2, ratio (L/H)}; R^2 = .998$	0.20	1.56	103.25±11.40
Pep-U3	$\log_2\text{Con}(\text{ng/ml}) = 4.039 + 1.023 * \log_2\text{Pep-U3, ratio (L/H)}; R^2 = .998$	0.84	1.15	100.42±9.48
Pep-U4	$\log_2\text{Con}(\text{ng/ml}) = 4.686 + 1.502 * \log_2\text{Pep-U4, ratio (L/H)}; R^2 = .998$	0.12	1.23	98.92±12.57
Pep-U5	$\log_2\text{Con}(\text{ng/ml}) = 3.099 + 1.056 * \log_2\text{Pep-U5, ratio (L/H)}; R^2 = .998$	0.57	1.79	100.69±12.22
Pep-US	$\log_2\text{Con, ng/ml} = 6.87 + .944 * \log_2\text{Pep-US, ratio (L/H)}; R^2 = .999$	14.46	2.04	114.21±6.07
Pep-UF	$\log_2\text{Con}(\text{ng/ml}) = 5.732 + .958 * \log_2\text{Pep-UF, ratio (L/H)}; R^2 = .998$	7.09	9.91	100.25±7.22

^a Linearity was determined by linear regression between measured concentration and peak area ratio (L/H) versus theoretical concentration determined by Light-SIS peptides (unlabeled form). All output of MultiQuant were weighted by $1/\chi^2$. Sum of all transition peak area ratio (L/H) to get peak area ratio at the peptide level.

^b LOQ was determined from the standard curve, defined as the lowest limits of quantification calibrated with acceptable CV<20% and accuracy within 100±20%.

^c Accuracy was estimated by back fitting data to the STD curve and average recovery from all quantified points in the plots. Data are mean±SD (%). Calibration curve is based on internal standard (IS unlabeled form) concentration and peak area ratio (transition ion peak area/IS peak area) and prepared in a pooled plasma matrix which was prepared from studying plasma samples >=5 points.

Sample preparation and SRM-MS analysis

Under a stereo microscope, approximately 200 intact islets from individual donors were handpicked into a polypropylene tube containing 1 ml of ice-cold PBS. After washing twice with 1 ml PBS containing 1X protease inhibitor cocktails, the islets were resuspended in 100 µl of 0.1% RapiGest (w/v) (Waters Corp., Milford, MA) containing 100 mM Tris-HCl (pH 8.0) and 100 nM DTT. For choroid plexus postmortem frozen sections 100 µl of 0.1% RapiGest was added on each slide, and then tissue was scraped off into a clean 1.5 ml of tube. Then, islet and choroid plexus in 0.1% RapiGest were sonicated 3 x 3 seconds on/30 seconds off on ice. After centrifugation (16,000g, 20 min at 4°C), supernatants were collected and protein concentration was determined by BCA assay (Cat#: 23225, Thermo Fisher Scientific, Waltham, MA), and stored at -80°C until further

analysis. Due to very low amounts of islet lysate, the islet protein concentration was not determined, and thus relative quantification was used for quantification, e.g., the ratio of pep-C α K/pep-C α and pep-Us/pep-B2.

Fresh-frozen human plasma was thawed on the day of analysis. After centrifugation (16,000g, 15 min at 4°C), cleared fractions were transferred with a loading tip into a fresh 1.5 mL polypropylene tube, discarding insoluble aggregates and the upper layer of floating lipids. This procedure was enough to eliminate the confounding influence of lipids on downstream protein separation procedures. Then 5 μ l of delipidated plasma was mixed with 95 μ l of 0.1% RapiGest.

Tryptic digestion was performed with an automated robotic procedure aimed at minimizing sample handling variability in a flow for SRM analysis(1). Briefly, sample lysate (100 μ l) in 0.1% RapiGest were transferred into the reaction plate, incubated 1 hour at 55°C for denaturation and reduction, followed by 30 min alkylation with a fresh made 0.1 M solution of iodoacetamide (Sigma-Aldrich) to a final concentration of 50 mM at room temperature in the dark. After alkylation, trypsin/LysC mix (Promega, Madison, WI) was added at an enzyme-to-substrate ratio of 1:50. Digestion was carried out for 18 hours at 37°C and terminated with 10% MS-grade trifluoroacetic acid (Fisher Scientific, Hampton, NH) to a final concentration of 1%. Acidified tryptic digests were cleaned up with 96-well SPE plate (Phenomenex, Torrance, CA) according to manufacturer's instruction. A 96-well plate vacuum manifold (Waters Corp., Milford, MA) was used for all desalting procedures to provide uniform peptide wash, retention, and elution. The elution reagents were evaporated to dryness and stored at -80°C until SRM analysis. All internal standard peptides of the novel *INS* uORF isoforms (INSU1 and INSU2) were post-spiked into tryptic digests. the tryptic pep-U3 is measured and validated by SRM-MS because the arginine digestion site (0) is flanked by prolines at -1 (promoting) and +1 (inhibiting) sites (2; 3).

We used a Shimadzu LC-HPLC equipped with LC-20ADXR pumps (Shimadzu Corp., Columbia, MD) for solvent and sample delivery and a 2.1 mm X 100 mm, 130 Å pore size, 3.5 μ m particle size C18 column (Waters Corp.) for the peptide separations using the following linear gradient: 0min 5%B; 10 min 36%B; 12 min 90%B; 13.5 min 90%B; 14 min 5%B at a flow rate of 0.2ml/min. The total run time was 18 min per sample. Triplicate injections of 10 μ l of sample were carried out via the SIL-20AXR autosampler (Shimadzu Corp.). To eliminate possible carryover, the column was re-equilibrated at 50%B for 10 min and a blank run was performed prior to initiating the next sample injection. QTRAP 5500 mass spectrometer with electrospray ionization (ESI) source controlled by Analyst 1.6.3 software (AB Sciex, Framingham, MA) was used for all LC-MS/MS detection and analysis. Mass spectrometric analyses were performed in positive ion mode. ESI interface parameters were set as follows: capillary temperature 650°C and a curtain gas setting of 30 psi. By using scheduled SRM, a total of 148 SRM transitions from 15 peptides were monitored during an individual sample analysis with Q1 and Q3 set by declustering potential (DE) 10 V and peptide-specific tuned collision energy (CE), entrance potential (EP) and collision cell exit (CXP) voltages for each transition.

1. Zhu M, Zhang P, Geng-Spyropoulos M, Moaddel R, Semba RD, Ferrucci L: A robotic protocol for high-throughput processing of samples for selected reaction monitoring assays. *Proteomics* 2017;17
2. Eisenhaber F, Eisenhaber B, Kubina W, Maurer-Stroh S, Neuberger G, Schneider G, Wildpaner M: Prediction of lipid posttranslational modifications and localization signals from protein sequences: big-Pi, NMT and PTS1. *Nucleic Acids Res* 2003;31:3631-3634
3. Pan Y, Cheng K, Mao J, Liu F, Liu J, Ye M, Zou H: Quantitative proteomics reveals the kinetics of trypsin-catalyzed protein digestion. *Anal Bioanal Chem* 2014;406:6247-6256